Methodol Comput Appl Probab (2019) 21:1–23
https://doi.org/10.1007/s11009-018-9638-z

First Hitting Time Distributions for Brownian Motion and Regions with Piecewise Linear Boundaries

Qinglai Dong[1,2] · **Lirong Cui**[1]

Received: 8 June 2017 / Revised: 10 April 2018 /
Accepted: 10 April 2018 / Published online: 25 April 2018

Abstract Explicit formulas for the first hitting time distributions for a standard Brownian motion and different regions including rectangular, triangle, quadrilateral and a region with piecewise linear boundaries are derived. Moreover, approximations to the first hitting time distribution of a standard Brownian motion with respect to regions with general nonlinear continuous boundaries are also obtained. The rules for assessing the accuracies of the approximations are given. We generalize the results of one-sided boundaries which include the general nonlinear continuous boundaries, piecewise linear boundaries, linear boundaries and constant boundaries to a region and give the relationships among the first hitting time distributions. Some numerical examples are presented to illustrate the results obtained in the paper. These formulas can be further extended to compute the first hitting time distributions of a Brownian motion with linear drift with respect to regions.

Keywords Brownian motion · First hitting time · Distribution · Region

Mathematics Subject Classification (2010) Primary 60J65, 60J75 · Secondary 60J60, 60J70

This work was supported by the National Natural Science Foundation of China under Grant 71631001.

✉ Qinglai Dong
Qinglaidong@163.com

[1] School of Management & Economics, Beijing Institute of Technology, Beijing, China

[2] School of Mathematics & Computer Science, Yanan University, Shaanxi, China

1 Introduction

Let $B(t), t \geq 0$ be a standard Brownian motion with $E[B(t)] = 0$, $E[B(t)B(s)] = \min(t, s)$ and D be a set. The first hitting time of $B(t)$ with respect to D is defined as

$$\tau_D = \begin{cases} \inf\{t \geq 0;\, B(t) \in D\}, & \text{if such } t \text{ exists,} \\ \infty, & \text{otherwise.} \end{cases} \tag{1}$$

The first hitting time distributions or boundary crossing probabilities of stochastic processes have been widely used in many fields, special for Brownian motion, for example, in finance, economics, business and management, and reliability engineering, for example, Cui et al. (2016), Dong and Cui (2017), and Gao et al. (2017) and Kong et al. (2017) and Wang et al. (2018) and Zhao et al. (2018). However, the calculation of the first hitting time distributions is not an easy task in which the related research has been done for many decades, for example, Jin and Wang (2017), Fu and Wu (2010), Che and Dassios (2013), and Herrmann and Tanré (2016) and so on. In general, there are many different kinds of boundaries, for example, constant boundaries, linear boundaries, piecewise linear boundaries (or polygonal boundaries), nonlinear boundaries and stochastic boundaries. In addition, according to the number of boundaries, there are also one-sided boundaries and multi-sided boundaries.

In almost any textbook about the Brownian motion, we can find the explicit formula for the constant boundary, and the first hitting time to the constant boundary follows an inverse Gaussian distribution (for example, Cox and Miller (1977)), i.e.,

$$P\{\tau_c \leq t\} = 2\left(1 - \Phi\left(\frac{c}{\sqrt{t}}\right)\right) = \sqrt{\frac{2}{\pi}} \int_{c/\sqrt{t}}^{\infty} e^{-\frac{x^2}{2}} dx, \tag{2}$$

where c is a constant, τ_c is the first hitting time to constant boundary c, and $\Phi(x)$ is a standard normal distribution function.

Doob (1949) is the first author who gave an explicit representation for the distribution of the first passage time of a Brownian motion through linear boundaries. If a linear boundary $c(t) = \alpha t + \beta$ with $\beta > 0$, the first hitting time distribution has simple closed-form expression Karatzas and Shreve (1991)

$$P\{\tau_c \leq t\} = 1 - \Phi\left(\frac{\alpha t + \beta}{\sqrt{t}}\right) + \exp(-2\alpha\beta)\Phi\left(\frac{\alpha t - \beta}{\sqrt{t}}\right). \tag{3}$$

For the piecewise linear boundary $c(s)$ which is defined on the partition $(t_i)_{i=1}^n$ of $[0, t]$ and satisfies $\lim_{s \to 0+} c(s) = c(0) > 0$, using the well-known formula of the conditional crossing probability (Siegmund 1986; Jin and Wang 2017) gave the explicit formula of the first hitting time distribution

$$P\{\tau_c \leq t\} = 1 - E[g_n(B_{t_1}, B_{t_2}, \cdots, B_{t_n}; c)], \tag{4}$$

where

$$g_n(\mathbf{x}; c) = \prod_{i=1}^{n} I\{x_i < c_i\} \left\{1 - \exp\left(-\frac{2(c_{i-1}^+ - x_{i-1})(c_i^- - x_i)}{t_i - t_{i-1}}\right)\right\},$$

and $\mathbf{x} = (x_1, x_2, \cdots, x_n)$, $x_0 = 0$, $c_i^+ = \lim_{s \to 0+} c(t_i + s)$, $c_i^- = \lim_{s \to 0+} c(t_i - s)$, $c_i = \min\{c_i^+, c_i^-\}$,

$c_0 = c_0^+ = c(0)$, $c_n = c_n^- = c(t)$,and $I\{A\}$ is an indicator function of event A, i.e., $I\{A\} = 1$, if Aoccurs, otherwise $I\{A\} = 0$, E is an expectation operator. The formulas

apply to continuous as well as discontinuous boundaries, and they are an extension of the results of continuous boundaries (Wang and Pötzelberger 1997).

For the nonlinear boundaries, explicit formulas exist only in a few special cases Novikov et al. (1999) and Daniels (1969). For example, analytic expressions involving hypergeometric functions are given in Novikov et al. (1999) for densities of the first hitting times $\inf\{t \geq 0 : B_t \geq \kappa + \eta\sqrt{\gamma + t}\}$ and $\inf\{t \geq 0 : |B_t| \geq \eta\sqrt{\gamma + t}\}$. To deal with general nonlinear boundaries, many scholars have been devoting themselves to looking for workable approximate solutions which can be applied without too much effort to a variety of situations. The traditional method is based on partial differential equations for the transition density function and focuses on approximate solutions of certain integral or differential equations for the first passage time densities, for example, the tangent approximation and other image methods (Strassen 1967; Daniels 1996), series expansion method (Durbin 1971; Ferebee 1983; Durbin and Williams 1992), and Monte Carlo path-simulation method (Giraudo and Sacerdote 1999; Giraudo et al. 2001). Another approach is based on the stochastic differential equation for the processes (Wang and Pötzelberger 2007; Molini et al. 2011). Exploiting the advantage of the finite Markov chain imbedding technique and the invariance principle, Fu and Wu (2010) provided a way to calculate the boundary crossing probabilities for linear and nonlinear boundaries by use of the multiplication of transition matrices. Moreover, see also Wang and Pötzelberger (2007), Jin and Wang (2017), and Herrmann and Tanré (2016) and references therein on the topic of approximations of the first passage distribution or the first passage density.

Most of the results above are about one-sided boundaries, there are also some results about two-sided boundaries, we can refer to Daniels (1996), Donchev (2010), Novikov et al. (1999), Abundo (2002), Pötzelberger and Wang (2001), and Wang and Pötzelberger (2007)) and references therein on the topic of the boundary crossing probabilities for a Brownian motion with two-sided boundaries. Moreover, the results above are all involving deterministic boundaries, we can refer to Peškir and Shiryaev (1998), Vondraček (2000), and Che and Dassios (2013) and references therein on the boundary crossing probabilities for a Brownian motion with stochastic boundaries.

In this paper, we aim to find the explicit first hitting time distributions of a Brownian motion with respect to a region which may be a rectangular, triangle, quadrilateral or a region with piecewise linear boundaries. Using these formulas, we can obtain approximations to the first hitting time distribution of a Brownian motion with respect to regions with general nonlinear continuous boundaries. To the best of our knowledge, there has not any literature involved in this problem. The region is different from the above deterministic boundaries which share a common feature: the starting points of the boundaries are on the ordinate axis. Moreover, if we consider some special cases, the region reduces to the above deterministic one-sided boundaries. In other words, we extend the existing results to more general cases. In fact, there are some examples of practical applications which can be described by the above situations. For example, in finance, an investor holding an American-style option and seeking optimal value will exercise it before maturity under certain circumstances; therefore, the investor is more concerned about the probability of the market price of an American-style option being in a certain range over a period of time, i.e., the probability of the market price hitting a rectangular region. For another example, in pharmacokinetics, in order to reach a steady state of the drug plasma concentration, we are concerned about the time course of the drug concentration in plasma. That is to say, if we can grasp the metabolic regularity of a drug, we can determine the best dosing interval and dose to maximize its effectiveness. Therefore, it is important to obtain the probability of the drug plasma concentration being in a certain range over a period of time.

The remainder of this paper is organized as follows. In Section 2 we derive the explicit formulas of the first hitting time distributions of a standard Brownian motion and a region, including rectangular, triangle, quadrilateral and a region with piecewise linear boundaries. Using these formulas, the approximations to the first hitting time distribution of a standard Brownian motion with respect to regions with general nonlinear continuous boundaries are obtained. In Section 3, relationships among the formulas of the first hitting time distributions are discussed. Some numerical examples to illustrate the results obtained in the paper are presented in Section 4. Finally, in Section 5, conclusions are given.

2 First Hitting Time Distributions for Regions

In this section, we are focused on the explicit formulas for the first hitting time distributions of a Brownian motion and regions. The regions considered in this paper are on the right side of the ordinate axis; thus, they are different from the existing boundaries. However, a region will reduce to a one-sided boundary, if we choose suitable conditions. For example, if the left boundary of a rectangular region tends to the ordinate axis infinitely, and the lower boundary is above the horizontal axis and tends to infinity, it becomes a one-sided constant boundary. In the following, rectangular, triangle, quadrilateral, rhombus regions and regions with piecewise linear boundaries are considered. Moreover, the approximations to the first hitting time distribution of a standard Brownian motion with respect to regions with general nonlinear continuous boundaries are obtained.

2.1 Brownian Motion and Rectangular Regions

A rectangular region is described by

$$D_R := \{(t, X)|0 < a \leq t \leq b \leq \infty, c \leq X \leq d \leq \infty\},$$

where a, b, c and d are constants, and region D_R can be shown in Fig. 1. Broadly speaking, if $b = \infty$ or $d = \infty$, it is also thought of as a rectangular region.

Our purpose is to calculate the first hitting time distribution of a standard Brownian motion and region D_R, i.e. $P\{\tau_{D_R} \leq t\}$, and we have the following result.

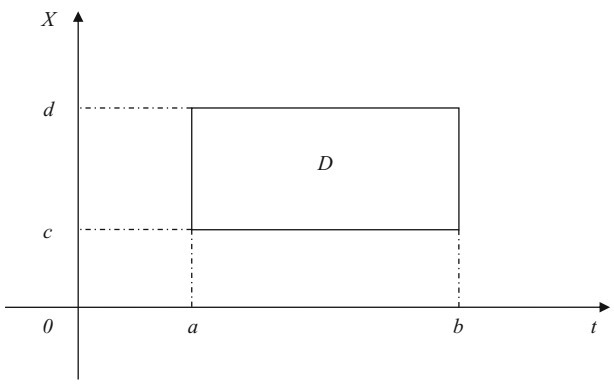

Fig. 1 A rectangular region

Theorem 1 *For any $t > 0$ and rectangular region D_R, the first hitting time distribution is given by*

$$P\{\tau_{D_R} \le t\} = \begin{cases} 0, & t < a \\ \Phi\left(\frac{d}{\sqrt{a}}\right) - \Phi\left(\frac{c}{\sqrt{a}}\right), & t = a \\ F_R^B(t), & a < t \le b \\ F_R^B(b), & b < t < \infty \end{cases} \tag{5}$$

$$P(\tau_{D_R} = \infty) = 1 - F_R^B(b),$$

where

$$\begin{aligned} F_R^B(t) \;=\; & 1 - \int_{-\infty}^{c}\int_{-\infty}^{c}\left[1 - \exp\left(-\frac{2(c-x)(c-y)}{t-a}\right)\right] \\ & \times \frac{1}{2\pi\sqrt{a(t-a)}} \exp\left(-\frac{1}{2}\left(\frac{x^2}{a} + \frac{(y-x)^2}{t-a}\right)\right) dxdy \\ & - \int_{-\infty}^{-d}\int_{-\infty}^{-d}\left[1 - \exp\left(-\frac{2(d+x)(d+y)}{t-a}\right)\right] \\ & \times \frac{1}{2\pi\sqrt{a(t-a)}} \exp\left(-\frac{1}{2}\left(\frac{x^2}{a} + \frac{(y-x)^2}{t-a}\right)\right) dxdy. \end{aligned}$$

Proof By the continuity of Brownian motion, there are only three ways for the sample path of a Brownian motion to hit the region, that is, the left boundary, the upper boundary and the lower boundary.

When $t < a$, we have

$$P\{\tau_{D_R} \le t\} = 0.$$

When $t = a$,

$$P\{\tau_{D_R} \le t\} = P\{\tau_{D_R} = a\} = P\{c \le B(a) \le d\} = \Phi\left(\frac{d}{\sqrt{a}}\right) - \Phi\left(\frac{c}{\sqrt{a}}\right) := p_1^R(t).$$

When $a < t \le b$, we can consider it in two cases:

(i) If $B(a) < c$, it then follows that

$$\begin{aligned} & P\{\tau_{D_R} \le t,\, B(a) < c\} \\ & = P\{B(a) < c\} - P\{\tau_{D_R} > t,\, B(a) < c\} \\ & = P\{B(a) < c\} - P\{B(s) < c, \forall s \in [a,t]\} \\ & = P\{B(a) < c\} - E\{P\{B(s) < c, \forall s \in [a,t] | B(a), B(t)\}\} \\ & = \Phi\left(\frac{c}{\sqrt{a}}\right) - E\left\{I\{B(a) < c\} I\{B(t) < c\}\left[1 - \exp\left(-\frac{2(c-B(a))(c-B(t))}{t-a}\right)\right]\right\} \\ & = \Phi\left(\frac{c}{\sqrt{a}}\right) - \int_{-\infty}^{c}\int_{-\infty}^{c}\left[1 - \exp\left(-\frac{2(c-x)(c-y)}{t-a}\right)\right] \\ & \times \frac{1}{2\pi\sqrt{a(t-a)}} \exp\left(-\frac{1}{2}\left(\frac{x^2}{a} + \frac{(y-x)^2}{t-a}\right)\right) dxdy \\ & := p_2^R(t), \end{aligned}$$

where the fourth equality follows from the well-known formula of the conditional crossing probability (Siegmund (1986)).

(ii) If $B(a) > d$, using the same method as (i), we have

$$\begin{aligned}
&P\{\tau_{D_R} \le t, B(a) > d\} \\
&= P\{B(a) > d\} - P\{\tau_{D_R} > t, B(a) > d\} \\
&= P\{B(a) > d\} - P\{-B(s) < -d, \forall s \in [a,t]\} \\
&= 1-\Phi\left(\frac{d}{\sqrt{a}}\right) - E\left\{I\{B(a)<-d\}I\{B(t)<-d\}\left[1-\exp\left(-\frac{2(d+B(a))(d+B(t))}{t-a}\right)\right]\right\} \\
&= 1-\Phi\left(\frac{d}{\sqrt{a}}\right) - \int_{-\infty}^{-d}\int_{-\infty}^{-d}\left[1-\exp\left(-\frac{2(d+x)(d+y)}{t-a}\right)\right] \\
&\quad \times \frac{1}{2\pi\sqrt{a(t-a)}}\exp\left(-\frac{1}{2}\left(\frac{x^2}{a}+\frac{(y-x)^2}{t-a}\right)\right)dxdy \\
&:= p_3^R(t),
\end{aligned}$$

where the third equality follows from the symmetry of Brownian motion. Consequently, for any $t \in (a,b]$, the expression of $F_R^B(t)$ is obtained by using

$$P\{\tau_{D_R} \le t\} = p_1^R(t) + p_2^R(t) + p_3^R(t) := F_R^B(t).$$

When $b < t < \infty$, because $P\{b < \tau_{D_R} \le t\} = 0$, we obtain

$$P\{\tau_{D_R} \le t\} = P\{\tau_{D_R} \le b\} + P\{b < \tau_{D_R} \le t\} = P\{\tau_{D_R} \le b\} = F_R^B(b).$$

Because the event $\{\tau_{D_R} = \infty\}$ stands for the fact that the sample path of a Brownian motion cannot hit the region forever,

$$P\{\tau_{D_R} = \infty\} = 1 - F_R^B(b).$$

The theorem follows. □

Moreover, when $a \to 0, b = \infty, c > 0$, the problem of rectangular region D_R reduces to that of a one-sided constant boundary. From the continuity of Brownian motion, $\lim_{a\to 0} B(a) = 0$. It follows Eq. 5 that

$$\begin{aligned}
\lim_{a\to 0} F_R^B(t) &= \lim_{a\to 0}\left\{1-E\{I\{B(a)<c\}I\left\{B(t)<c\right\}\left[1-\exp\left(-\frac{2(c-B(a))(c-B(t))}{t-a}\right)\right]\right\} \\
&\qquad -E\left\{I\left\{B(a)<-d\right\}I\{B(t)<-d\}\left[1-\exp\left(-\frac{2(d+B(a))(d+B(t))}{t-a}\right)\right]\right\}\Bigg\} \\
&= 1-E\left\{I\{B(t)<c\}\left[1-\exp\left(-\frac{2c(c-B(t))}{t}\right)\right]\right\} \\
&= 1-\int_{-\infty}^{c}\left[1-\exp\left(-\frac{2c(c-y)}{t}\right)\right]\frac{1}{\sqrt{2\pi t}}\exp\left(-\frac{y^2}{2t}\right)dy \;= 2\left(1-\Phi\left(\frac{c}{\sqrt{t}}\right)\right).
\end{aligned}$$

The result is in line with Eq. 2. Furthermore,

$$P\{\tau_{D_R} = \infty\} = P\{\tau_c = \infty\} = \lim_{\substack{a \to 0 \\ b \to \infty}} (1 - F_R^B(b))$$
$$= \lim_{b \to \infty} \left(1 - 2\left(1 - \Phi\left(\frac{c}{\sqrt{b}}\right)\right)\right) = 1 - 2(1 - \Phi(0)) = 0$$

which leads to $P\{\tau_c < \infty\} = 1$. The result is same as that in Karatzas and Shreve (1991).

2.2 Brownian Motion and Quadrilateral Regions

A quadrilateral region can be divided into two types denoted by type-I and type-II, respectively, and they are shown in Fig. 2. Thus, the quadrilateral region can be described by

$$D_Q := \{(t, X) | 0 < a \le t \le b \le \infty, l_1(t) \le X \le l_2(t)\},$$

where $l_1(t)$ and $l_2(t)$ are linear functions in type-I region, and they are polygonal functions in type-II region. For simplicity, we use the same symbols to denote the boundaries of the regions, and type-I and type-II regions are denoted by D_{Q_I} and $D_{Q_{II}}$, respectively.

The biggest difference between the two types of regions is the ways for the sample path of Brownian motion to hit the region. For type-I region, there are three ways—the left boundary, the upper boundary and the lower boundary, whereas there are four ways for type-II region, that is, the sample path of Brownian motion can hit the region from four boundaries. In a type-I quadrilateral region, if $l_1(a) = l_2(a)$ or $l_1(b) = l_2(b)$, it reduces to a triangle region denoted by type-I, which is shown in Fig. 3. In a type-II quadrilateral region, if $l_1(t) \equiv c$ or $l_2(t) \equiv d$, it also reduces to a triangle region denoted by type-II, which is shown in Fig. 4. We first calculate the first hitting time distribution of a standard Brownian motion and type-I region D_{Q_I}, and we have the following result.

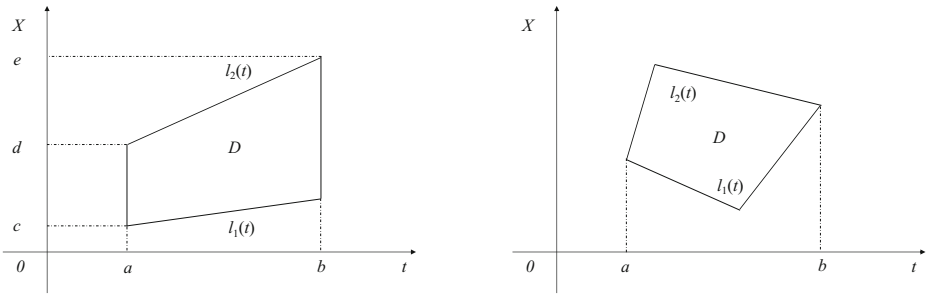

(a) A type-I quadrilateral region

(b) A type-II quadrilateral region

Fig. 2 Quadrilateral regions

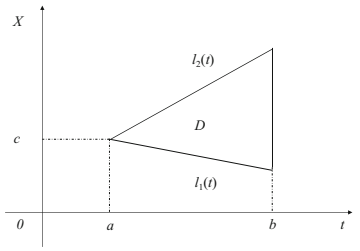

(a) A special case of type-I quadrilateral region for $l_1(a)=l_2(a)$

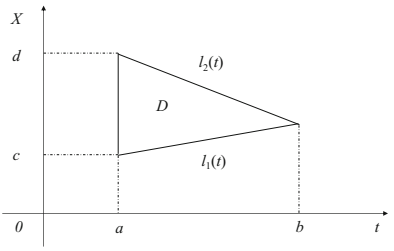

(b) A special case of type-I quadrilateral region for $l_1(b)=l_2(b)$

Fig. 3 Type-I triangle regions

Theorem 2 *For any $t > 0$ and type-I quadrilateral region D_{Q_I}, the first hitting time distribution of a standard Brownian motion is given by*

$$P\{\tau_{D_{Q_I}} \le t\} = \begin{cases} 0, & t < a \\ \Phi\left(\frac{l_2(a)}{\sqrt{a}}\right) - \Phi\left(\frac{l_1(a)}{\sqrt{a}}\right), & t = a \\ F^B_{Q_I}(t), & a < t \le b \\ F^B_{Q_I}(b), & b < t < \infty \end{cases} \tag{6}$$

$$P\{\tau_{D_{Q_I}} = \infty\} = 1 - F^B_{Q_I}(b),$$

where

$$\begin{aligned} F^B_{Q_I}(t) \;=\; & 1 - \int_{-\infty}^{l_1(t)} \int_{-\infty}^{l_1(a)} \left[1 - \exp\left(-\frac{2(l_1(a)-x)(l_1(t)-y)}{t-a}\right)\right] \\ & \times \frac{1}{2\pi\sqrt{a(t-a)}} \exp\left(-\frac{1}{2}\left(\frac{x^2}{a} + \frac{(y-x)^2}{t-a}\right)\right) dxdy \\ & - \int_{-\infty}^{-l_2(t)} \int_{-\infty}^{-l_2(a)} \left[1 - \exp\left(-\frac{2(l_2(a)+x)(l_2(t)+y)}{t-a}\right)\right] \\ & \times \frac{1}{2\pi\sqrt{a(t-a)}} \exp\left(-\frac{1}{2}\left(\frac{x^2}{a} + \frac{(y-x)^2}{t-a}\right)\right) dxdy. \end{aligned}$$

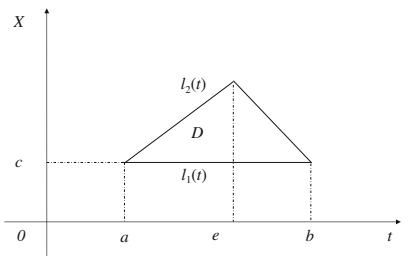

(a) A special case of type-II quadrilateral region for $l_1(t) \equiv c$

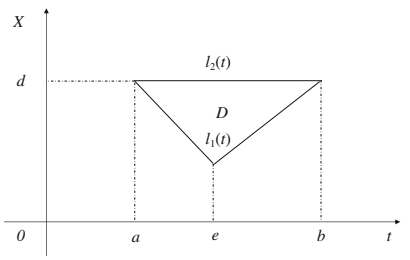

(b) A special case of type-II quadrilateral region for $l_2(t) \equiv d$

Fig. 4 Type-II triangle regions

Proof There are three ways—the left boundary, the upper boundary and the lower boundary for the sample path of Brownian motion to hit the region. Similar to Theorem 1,

$$p_1^{Q_I}(t) = \Phi\left(\frac{d}{\sqrt{a}}\right) - \Phi\left(\frac{c}{\sqrt{a}}\right) = \Phi\left(\frac{l_2(a)}{\sqrt{a}}\right) - \Phi\left(\frac{l_1(a)}{\sqrt{a}}\right) \text{ for } t = a.$$

$p_2^{Q_I}(t)$ and $p_3^{Q_I}(t)$ follow from Eq. 4 that, for any $t \in (a, b]$,

$$\begin{aligned} p_2^{Q_I} &= \Phi\left(\frac{l_1(a)}{\sqrt{a}}\right) - \int_{-\infty}^{l_1(t)} \int_{-\infty}^{l_1(a)} \left[1 - \exp\left(-\frac{2(l_1(a)-x)(l_1(t)-y)}{t-a}\right)\right] \\ &\quad \times \frac{1}{2\pi\sqrt{a(t-a)}} \exp\left(-\frac{1}{2}\left(\frac{x^2}{a} + \frac{(y-x)^2}{t-a}\right)\right) dxdy, \end{aligned}$$

$$\begin{aligned} p_3^{Q_I} &= 1 - \Phi\left(\frac{l_2(a)}{\sqrt{a}}\right) - \int_{-\infty}^{-l_2(t)} \int_{-\infty}^{-l_2(a)} \left[1 - \exp\left(-\frac{2(l_2(a)+x)(l_2(t)+y)}{t-a}\right)\right] \\ &\quad \times \frac{1}{2\pi\sqrt{a(t-a)}} \exp\left(-\frac{1}{2}\left(\frac{x^2}{a} + \frac{(y-x)^2}{t-a}\right)\right) dxdy. \end{aligned}$$

Therefore, if $a < t \le b$, the expression of $F_{Q_I}^B(t)$is obtained by using

$$P\{\tau_{D_{Q_I}} \le t\} = p_1^{Q_I}(t) + p_2^{Q_I}(t) + p_3^{Q_I}(t) := F_{Q_I}^B(t).$$

Therefore, Eq. 6 follows from the same method as Theorem 1 and the above results. □

It is easily seen that Eq. 6 is exactly (5) for $l_1(t) \equiv c$ and $l_2(t) \equiv d$. Moreover, if $l_1(a) = l_2(a)$, it reduces to a triangle region (Fig. 3a), the first hitting time distribution has the same expression as Eq. 6 instead of $p_1^{Q_I}(t) = 0$. If $l_1(b) = l_2(b)$, it also reduces to a triangle region (Fig. 3b), and the first hitting time distribution has the same expression as Eq. 6.

Because the boundaries of type-II quadrilateral regions are polygonal functions, we first consider the region with piecewise linear boundaries, and then give the relevant result as a special case.

2.3 Brownian Motion and Regions with Piecewise Linear Boundaries

A region with piecewise linear boundaries is described by

$$D_{PL} := \{(t, X) | 0 < a \le t \le b \le \infty, l_1(t) \le X \le l_2(t)\}$$

where $l_1(t)$ and $l_2(t)$ are polygonal functions on $[a, b]$, $l_1(a) = c, l_2(a) = d$, and it is shown in Fig. 5.

Let $a = t_0 < t_1 < \cdots < t_n = t \le t_{n+1} \le \cdots \le t_m = b$ be a partition of $[a, b]$ of size $m \ge 1$, $l_1(s)$ and $l_2(s)$ be linear functions on each intervals $[t_{i-1}, t_i]$, $i = 1, 2, \cdots, m$. We have the following result about the first hitting time distribution of a standard Brownian motion and region D_{PL}.

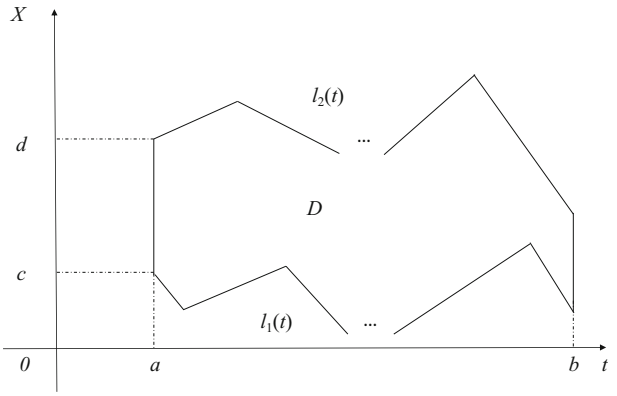

Fig. 5 A region with piecewise linear boundaries

Theorem 3 *For any $t > 0$ and region D_{PL}, the first hitting time distribution of a standard Brownian motion is given by*

$$P\{\tau_{D_{PL}} \le t\} = \begin{cases} 0, & t < a \\ \Phi\left(\frac{l_2(a)}{\sqrt{a}}\right) - \Phi\left(\frac{l_1(a)}{\sqrt{a}}\right), & t = a \\ F^B_{PL}(t), & a < t \le b \\ F^B_{PL}(b), & b < t < \infty \end{cases} \tag{7}$$

$$P\{\tau_{D_{PL}} = \infty\} = 1 - F^B_{PL}(b),$$

where

$$\begin{aligned} F^B_{PL} = 1 &- \int_{-\infty}^{l_1(t_n)} \int_{-\infty}^{l_1(t_{n-1})} \cdots \int_{-\infty}^{l_1(a)} \prod_{i=1}^{n} \left[1 - \exp\left(-\frac{2(l_1(t_{i-1}) - x_{i-1})(l_1(t_i) - x_i)}{t_i - t_{i-1}}\right)\right] \\ &\times \frac{1}{(2\pi)^{\frac{n+1}{2}} \left(a \prod_{i=1}^{n} (t_i - t_{i-1})\right)^{\frac{1}{2}}} \exp\left(-\frac{1}{2}\left(\frac{x_0^2}{a} + \frac{(x_1 - x_0)^2}{t_1 - a} + \cdots + \frac{(x_n - x_{n-1})^2}{t_n - t_{n-1}}\right)\right) dx_0 dx_1 \cdots dx_n \\ &- \int_{-\infty}^{-l_2(t_n)} \int_{-\infty}^{-l_2(t_{n-1})} \cdots \int_{-\infty}^{-l_2(a)} \prod_{i=1}^{n} \left[1 - \exp\left(-\frac{2(l_2(t_{i-1}) + x_{i-1})(l_2(t_i) + x_i)}{t_i - t_{i-1}}\right)\right] \\ &\times \frac{1}{(2\pi)^{\frac{n+1}{2}} \left(a \prod_{i=1}^{n} (t_i - t_{i-1})\right)^{\frac{1}{2}}} \exp\left(-\frac{1}{2}\left(\frac{x_0^2}{a} + \frac{(x_1 - x_0)^2}{t_1 - a} + \cdots + \frac{(x_n - x_{n-1})^2}{t_n - t_{n-1}}\right)\right) dx_0 dx_1 \cdots dx_n. \end{aligned}$$

Proof Although the upper and lower boundaries are polygonal functions, there are only three ways for the sample path of Brownian motion to hit the region, i.e., the left boundary, the upper boundary and the lower boundary; thus, we only need to calculate $p_1^{PL}(t)$, $p_2^{PL}(t)$ and $p_3^{PL}(t)$. Similar to Theorem 1,

$$p_1^{PL}(t) = \Phi\left(\frac{l_2(a)}{\sqrt{a}}\right) - \Phi\left(\frac{l_1(a)}{\sqrt{a}}\right).$$

$p_2^{PL}(t)$ and $p_3^{PL}(t)$ follow from Eq. 4 that, for any $t \in (a, b]$,

$$p_2^{PL}(t) = \Phi\left(\frac{l_1(a)}{\sqrt{a}}\right) - E\left\{\prod_{i=1}^{n} I\{B(t_{i-1}) < l_1(t_{i-1})\} I\{B(t_i) < l_1(t_i)\} \times \left[1 - \exp\left(-\frac{2(l_1(t_{i-1}) - B(t_{i-1}))(l_1(t_i) - B(t_i))}{t_i - t_{i-1}}\right)\right]\right\},$$

$$p_3^{PL} = 1 - \Phi\left(\frac{l_2(a)}{\sqrt{a}}\right) - E\left\{\prod_{i=1}^{n} I\{B(t_{i-1}) < -l_2(t_{i-1})\} I\{B(t_i) < -l_2(t_i)\} \times \left[1 - \exp\left(-\frac{2(l_2(t_{i-1}) + B(t_{i-1}))(l_2(t_i) + B(t_i))}{t_i - t_{i-1}}\right)\right]\right\}.$$

Therefore, if $a < t \le b$, the expression of $F_{PL}^B(t)$ is obtained by using integration and

$$P\{\tau_{D_{PL}} \le t\} = p_1^{PL}(t) + p_2^{PL}(t) + p_3^{PL}(t) := F_{PL}^B(t).$$

The theorem follows. □

Using Eq. 7, we can obtain the first hitting time distributions of some special cases. Because $F_{PL}^B(t)$ is the main contributor to Eq. 7, we only need to consider the expressions of $F_{PL}^B(t)$ in the following cases.

Special case 1: Quadrilateral regions (type-I) If $l_1(t)$ and $l_2(t)$are linear functions, region D_{PL} reduces to a type-I quadrilateral region D_{Q_I} as shown in Fig. 2a. By using Eq. 7 and $n = 1$, we obtain the same result in Theorem 2.

Special case 2: Quadrilateral regions (type-II) If $l_1(t)$ and $l_2(t)$ have only two segments, respectively, D_{PL} reduces to a hexagon; moreover, if $l_1(a) = l_2(a)$ and $l_1(b) = l_2(b)$ are added, D_{PL} reduces to a type-II quadrilateral region as shown in Fig. 2b. The expression of $F_{Q_{II}}^B(t)$ can be easily obtained by letting $n = 3$ in (7).

Special case 3: Rhombus regions If the region is a rhombus which is a special case of type-II quadrilateral regions and shown in Fig. 6. It follows from Eq. 7, $n = 2$ and $t_1 = e$ that

$$\begin{aligned} F_{RH}^B(t) = 1 &- \int_{-\infty}^{l_1(t)} \int_{-\infty}^{l_1(e)} \int_{-\infty}^{l_1(a)} \left[1 - \exp\left(-\frac{2(l_1(a) - x)(l_1(e) - y)}{e - a}\right)\right] \\ &\times \left[1 - \exp\left(-\frac{2(l_1(e) - y)(l_1(t) - z)}{t - e}\right)\right] \\ &\times \frac{1}{(2\pi)^{\frac{3}{2}}\sqrt{a(e-a)(t-e)}} \exp\left(-\frac{1}{2}\left(\frac{x^2}{a} + \frac{(y-x)^2}{e-a} + \frac{(z-y)^2}{t-e}\right)\right) dxdydz \\ &- \int_{-\infty}^{-l_2(t)} \int_{-\infty}^{-l_2(e)} \int_{-\infty}^{-l_2(a)} \left[1 - \exp\left(-\frac{2(l_2(a) + x)(l_2(e) + y)}{e - a}\right)\right] \\ &\times \left[1 - \exp\left(-\frac{2(l_2(e) + y)(l_2(t) + z)}{t - e}\right)\right] \\ &\times \frac{1}{(2\pi)^{\frac{3}{2}}\sqrt{a(e-a)(t-e)}} \exp\left(-\frac{1}{2}\left(\frac{x^2}{a} + \frac{(y-x)^2}{e-a} + \frac{(z-y)^2}{t-e}\right)\right) dxdydz. \end{aligned}$$

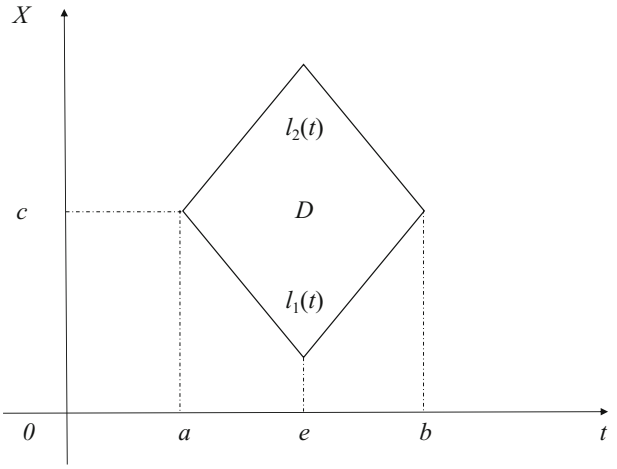

Fig. 6 A rhombus region

Special case 4: Triangle regions (type-II) A triangle region (type-II) which is shown in Fig. 4a can be obtained by letting $l_1(t) \equiv c$, $l_2(t)$ be a polygonal function with two segments, and $l_2(a) = l_2(b) = c$. It follows from Eq. 7, $n = 2$ and $t_1 = e$ that

$$\begin{aligned} F^B_{T_l}(t) \;=\; & 1-\int_{-\infty}^{c}\int_{-\infty}^{c}\left[1-\exp\left(-\frac{2(c-x)(c-y)}{t-a}\right)\right]\times\frac{1}{2\pi\sqrt{a(t-a)}}\exp\left(-\frac{1}{2}\left(\frac{x^2}{a}+\frac{(y-x)^2}{t-a}\right)\right)dxdy \\ & -\int_{-\infty}^{-l_2(t)}\int_{-\infty}^{-l_2(e)}\int_{-\infty}^{-c}\left[1-\exp\left(-\frac{2(c+x)(l_2(e)+y)}{e-a}\right)\right]\times\left[1-\exp\left(-\frac{2(l_2(e)+y)(l_2(t)+z)}{t-e}\right)\right] \\ & \times\frac{1}{(2\pi)^{\frac{3}{2}}\sqrt{a(e-a)(t-e)}}\exp\left(-\frac{1}{2}\left(\frac{x^2}{a}+\frac{(y-x)^2}{e-a}+\frac{(z-y)^2}{t-e}\right)\right)dxdydz. \end{aligned}$$

Using the same method, we can get the formula for a triangle region (type-II) as shown in Fig. 4b.

Special case 5: One-Sided piecewise linear boundaries If we choose$a \to 0$, $b = \infty$ and $l_1(0) > 0$, D_{PL} reduces to a one-sided piecewise linear boundary. Similarly, it follows from Eq. 7 that

$$\begin{aligned} & \lim_{a\to 0} F^B_{PL}(t) = 1-\int_{-\infty}^{l_1(t_n)}\int_{-\infty}^{l_1(t_{n-1})}\cdots\int_{-\infty}^{l_1(t_1)}\prod_{i=1}^{n}\left[1-\exp\left(-\frac{2(l_1(t_{i-1})-x_{i-1})(l_1(t_i)-x_i)}{t_i-t_{i-1}}\right)\right] \\ & \times(2\pi)^{-\frac{n}{2}}\left(\prod_{i=1}^{n}(t_i-t_{i-1})\right)^{-\frac{1}{2}}\exp\left(-\frac{1}{2}\left(\frac{x_1^2}{t_1}+\frac{(x_2-x_1)^2}{t_2-t_1}+\cdots+\frac{(x_n-x_{n-1})^2}{t_n-t_{n-1}}\right)\right)dx_1\cdots dx_n, \end{aligned}$$

where $t_0 = 0$, $x_0 = 0$. The result is same as that in Wang and Pötzelberger (1997).

2.4 Brownian Motion and Regions with General Nonlinear Continuous Boundaries

In this section we will use Eq. 7 and the idea of approximation introduced by Wang and Pötzelberger (1997) to obtain an approximation to the first hitting time distribution of a standard Brownian motion with respect to regions with general nonlinear continuous boundaries.

A region with general nonlinear continuous boundaries is described by

$$D_{GN} := \{(t, X) | 0 < a \le t \le b \le \infty, l_1(t) \le X \le l_2(t)\}$$

where $l_1(t)$ and $l_2(t)$ are nonlinear continuous functions on $[a, b]$, $l_1(a) = c$, $l_2(a) = d$, and it is shown in Fig. 7. Assume that $l_1(t)$ and $l_2(t)$ can be uniformly approximated by two sequences of piecewise linear functions, respectively. We have the following result.

Theorem 4 *For any $t > 0$ and region D_{GN}, the first hitting time distribution of a standard Brownian motion is given by*

$$P\{\tau_{D_{GN}} \le t\} = \begin{cases} 0, & t < a \\ \Phi\left(\frac{l_2(a)}{\sqrt{a}}\right) - \Phi\left(\frac{l_1(a)}{\sqrt{a}}\right), & t = a \\ F^B_{GN}(t), & a < t \le b \\ F^B_{GN}(b), & b < t < \infty \end{cases} \tag{8}$$

$$P\{\tau_{D_{GN}} = \infty\} = 1 - F^B_{GN}(b),$$

where

$$\begin{aligned} F^B_{GN} = 1 &- \lim_{n_1 \to \infty} \int_{-\infty}^{l_1(t_{n_1})} \int_{-\infty}^{l_1(t_{n_1-1})} \cdots \int_{-\infty}^{l_1(a)} \prod_{i=1}^{n_1} \left[1 - \exp\left(-\frac{2(l_1(t_{i-1}) - x_{i-1})(l_1(t_i) - x_i)}{t_i - t_{i-1}}\right)\right] \\ &\times \frac{1}{(2\pi)^{\frac{n_1+1}{2}} \left(a \prod_{i=1}^{n_1} (t_i - t_{i-1})\right)^{\frac{1}{2}}} \exp\left(-\frac{1}{2}\left(\frac{x_0^2}{a} + \frac{(x_1 - x_0)^2}{t_1 - a} + \cdots + \frac{(x_{n_1} - x_{n_1-1})^2}{t_{n_1} - t_{n_1-1}}\right)\right) dx_0 dx_1 \cdots dx_{n_1} \\ &- \lim_{n_2 \to \infty} \int_{-\infty}^{-l_2(t_{n_2})} \int_{-\infty}^{-l_2(t_{n_2-1})} \cdots \int_{-\infty}^{-l_2(a)} \prod_{i=1}^{n_2} \left[1 - \exp\left(-\frac{2(l_2(t_{i-1}) + x_{i-1})(l_2(t_i) + x_i)}{t_i - t_{i-1}}\right)\right] \\ &\times \frac{1}{(2\pi)^{\frac{n_2+1}{2}} \left(a \prod_{i=1}^{n_2} (t_i - t_{i-1})\right)^{\frac{1}{2}}} \exp\left(-\frac{1}{2}\left(\frac{x_0^2}{a} + \frac{(x_1 - x_0)^2}{t_1 - a} + \cdots + \frac{(x_{n_2} - x_{n_2-1})^2}{t_{n_2} - t_{n_2-1}}\right)\right) dx_0 dx_1 \cdots dx_{n_2}. \end{aligned}$$

where for $i = 1, 2$, $a = t_0 < t_1 < \cdots < t_{n_i} = t \le t_{n_i+1} \le \cdots \le t_{m_i} = b$ are arbitrary partitions of $[a, b]$ with size $m_i \ge 1$, $l_1(s)$ and $l_2(s)$ are linear functions on each intervals $[t_{j-1}, t_j]$, $j = 1, 2, \cdots, m_i$.

Proof The result is easily obtained using Theorem 3 presented in the current paper and Theorem 2 given in Wang and Pötzelberger (1997). □

Remark Because a Brownian motion with linear drift inherits from a standard Brownian motion almost all the properties, explicit formulas of the first hitting time distribution of a

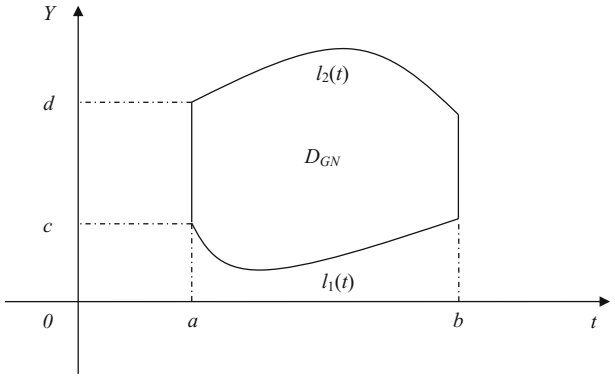

Fig. 7 A region with general nonlinear continuous boundaries

Brownian motion with linear drift with respect to regions can also be obtained by use of the formulas in Sections 2.1–2.4 and the transformations of boundaries.

3 Relationships of the First Hitting Time Distributions

In this section, we will consider the relationships of the first hitting time distributions. In fact, there are many special cases for a region with piecewise linear boundaries, for example, if $l_1(t)$ and $l_2(t)$ have only two segments, respectively, a region with piecewise linear boundaries becomes a hexagon region, if $l_1(a) = l_2(a)$ or $l_1(b) = l_2(b)$ is added, then it becomes the pentagon region, and if $l_1(a) = l_2(a)$ and $l_1(b) = l_2(b)$ are added, then it becomes the type-II quadrilateral region. Moreover, if $l_1(t)$ and $l_2(t)$ are all linear functions, a region with piecewise linear boundaries will become a quadrilateral region, and Theorem 3 reduces to Theorem 2; further, if $l_1(t)$ and $l_2(t)$ are all constants, the region will become a rectangular region, and Theorem 2 reduces to Theorem 1; even further, if we let $a \to 0$, $b = \infty$ and $c > 0$, Theorem 1 reduces to the result of a standard Brownian motion and one-sided constant boundary, and the first hitting time follows an inverse Gaussian distribution (Cox and Miller 1977). On the other hand, if we let $l_1(t)$ be a polygonal function, $a \to 0$, $b = \infty$ and $l_1(0) > 0$ for a standard Brownian motion and a region with piecewise linear boundaries, then it reduces to the problem of a standard Brownian motion and one-sided piecewise linear boundaries, and Theorem 3 reduces to the result of Wang and Pötzelberger (1997); moreover, if the boundary is a linear function in Wang and Pötzelberger (1997), it reduces to the case of a standard Brownian motion and one-sided linear boundaries (Doob 1949), which can also be obtained in the following way: if we let $a \to 0$, $b = \infty$ and $l_1(0) > 0$ for a standard Brownian motion and a quadrilateral region, i.e., Eq. 6 (Theorem 2) reduces to Eq. 2.

Figure 8 illustrates the relationships among theorems given in the paper and known results.

4 Numerical Examples

The calculation of the first hitting time distributions involves integral calculation of $\exp(-x^2/2)$ whose primitive function cannot always be expressed by an explicit formula

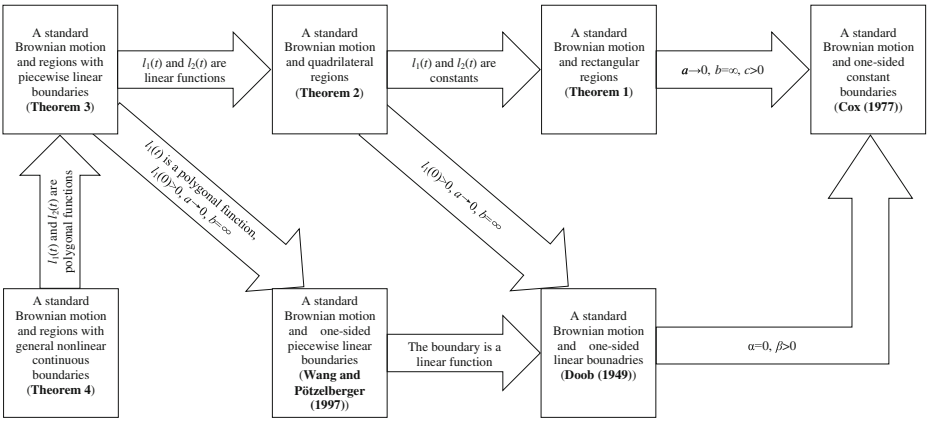

Fig. 8 Relationships of the first hitting time distributions

and hence must be calculated numerically. And it is straight forward by using the Monte Carlo integration method which has been proven to be an effective method, and the steps can be found in Ripley (1987) and Wang and Pötzelberger (1997). Moreover, the simulation precision can be assessed by the corresponding simulation standard error (Niederreiter 1992)

$$S = \sqrt{\frac{\sum [h(x) - \hat{J}]^2}{N(N-1)}}, \tag{9}$$

where $h(x)$ is the sample realization of the integrand, $\hat{J} = \sum h(x)/N$, and N is the simulation sample size. Therefore, the approximation error can be reduced by increasing the simulation size N. In all examples, we use simulation sample size $N = 2 \times 10^5$.

In the following, we calculate some examples to illustrate the results obtained in the paper. The numerical computations include the case of rectangle regions, the case of regions of piecewise linear boundaries and the case of general nonlinear continuous boundaries, while other cases can be done in the same way.

Firstly, we consider the case of rectangle regions. In order to explore the influence of regions on the first hitting time distribution, the cases of three fixed boundaries and a shifting boundary and the case of fixed area and variable position are used to illustrate the influence of position on the probability $P\{\tau_{D_R} \le b\}$.

Now, we calculate the probability $P\{\tau_{D_R} \le b\}$ with fixed $a = 2$, $b = 3$, $c = 0.2$ and different d for rectangle regions, and the numerical results are given in Table 1. The standard errors which can be calculated by using Eq. 9 are in parentheses. From Table 1, we can find that when $c = d = 0.2$, $p_1^R(t) = 0$, it can be explained by the fact that the probability of a standard Brownian motion hitting a region at one point is zero. In theory, when a, b and c are fixed, $p_2^R(t)$ will be a constant; however, in the row of $p_2^R(t)$, we find that some of them are slightly different from each other, it can be explained by the simulation errors. Moreover, the probability becomes more and more stable as d increases, that is, the probability that the sample path of a Brownian motion hits the region from the upper boundary tends to 0,

Table 1 $P\left\{\tau_{D_R} \leq b\right\}$ with fixed a, b, c and different d for rectangle regions(standard errors are in parentheses)

d	0.2	0.5	0.8	1	1.5	2	3	5	10
$P\left\{\tau_{D_R} \leq b\right\}$	0.390442	0.447478	0.499586	0.527669	0.583629	0.613690	0.642793	0.648041	0.647103
	(0.001872)	(0.001793)	(0.001698)	(0.001634)	(0.001471)	(0.001332)	(0.001123)	(0.000993)	(0.000978)
$p_1^R(t)$	0	0.081932	0.157965	0.204018	0.299346	0.365118	0.426821	0.443565	0.443768
$p_2^R(t)$	0.205999	0.204253	0.203648	0.203064	0.205008	0.202737	0.204849	0.204341	0.203334
	(0.000977)	(0.000978)	(0.000978)	(0.000979)	(0.000977)	(0.000979)	(0.000977)	(0.000978)	(0.000978)
$p_3^R(t)$	0.184443	0.161293	0.137972	0.120586	0.079275	0.045834	0.011122	1.352×10^{-4}	7.687×10^{-13}
	(0.000895)	(0.000815)	(0.000719)	(0.000654)	(0.000493)	(0.000353)	(0.000146)	(0.000015)	(0)

Table 2 $P\{\tau_{D_R} \leq b\}$ with fixed a, b, d and different c for rectangle regions(standard errors are in parentheses)

c	2	1.5	1	0.2	0.1	0	-1	-5	-10
$P\{\tau_{D_R} \leq b\}$	0.183177	0.287639	0.411736	0.613690	0.641336	0.660625	0.847399	0.967900	0.966903
	(0.001191)	(0.001307)	(0.001369)	(0.001332)	(0.001309)	(0.001296)	(0.001008)	(0.000358)	(0.000355)
$p_1^R(t)$	0	0.065772	0.161100	0.365118	0.393164	0.421350	0.681600	0.921147	0.921350
$p_2^R(t)$	0.137448	0.176035	0.204432	0.202737	0.201829	0.193480	0.119409	0.000168	7.687×10^{-13}
	(0.000837)	(0.000954)	(0.001018)	(0.000979)	(0.000960)	(0.000943)	(0.000657)	(9.65×10^{-6})	(0)
$p_3^R(t)$	0.045728	0.045831	0.045831	0.045834	0.046342	0.045794	0.046389	0.046585	0.045553
	(0.000354)	(0.000353)	(0.000351)	(0.000353)	(0.000349)	(0.000353)	(0.000351)	(0.000348)	(0.000355)

Table 3 $P\{\tau_{D_R} \leq b\}$ with fixed a, c, d and different b for rectangle regions(standard errors are in parentheses)

b	1	1.5	2	5	10	10^2	10^3	10^5	10^{12}
$P\{\tau_{D_R} \leq b\}$	0.136290	0.333126	0.414907	0.619292	0.728699	0.913449	0.972485	0.997247	0.999999
	(0.001152)	(0.001145)	(0.001119)	(0.000964)	(0.000799)	(0.000347)	(0.000124)	(0.000013)	(4.1×10^{-9})
$p_1^R(t)$	0.135905	0.135905	0.135905	0.135905	0.135905	0.135905	0.135905	0.135905	0.135905
$p_2^R(t)$	0.000554	0.182692	0.262167	0.463923	0.572108	0.755482	0.814051	0.838613	0.841343
	(0.000818)	(0.000970)	(0.000979)	(0.000875)	(0.000738)	(0.000325)	(0.000116)	(0.000012)	(3.9×10^{-9})
$p_3^R(t)$	0	0.014528	0.016834	0.019463	0.020685	0.022061	0.022528	0.022728	0.022751
		(0.000175)	(0.000140)	(0.000088)	(0.000061)	(0.000022)	(0.000007)	(7.3×10^{-7})	(2.3×10^{-10})

Table 4 $P\{\tau_{D_R} \leq b\}$ with fixed area and different positions for rectangle regions(standard errors are in parentheses)

(a, c)	(0.1, -2)	(0.1,-0.5)	(0.1,2)	(1,-2)	(1,-0.5)	(1,2)	(10,-2)	(10,-0.5)	(10,2)
$P\{\tau_{D_R} \leq b\}$	0.3407	0.987877	0.056305	0.415912	0.739583	0.150038	0.282281	0.311018	0.235452
	(0.000838)	(0.000217)	(0.000425)	(0.001125)	(0.001312)	(0.000731)	(0.001916)	(0.002042)	(0.001719)
$p_1^R(t)$	7.827×10^{-4}	0.886153	1.27×10^{-10}	0.135905	0.382924	0.021403	0.112371	0.125632	0.092153
$p_2^R(t)$	1.27×10^{-10}	0.050869	0.056305	0.016440	0.177931	0.127634	0.072277	0.093125	0.090995
	(0)	(0.000108)	(0.000425)	(0.000144)	(0.000656)	(0.000699)	(0.000842)	(0.001021)	(0.001028)
$p_3^R(t)$	0.3400	0.050854	0	0.26356	0.178728	0.00101	0.097633	0.092259	0.052304
	(0.000838)	(0.000109)	(0)	(0.000981)	(0.000655)	(0.000032)	(0.001073)	(0.001021)	(0.000691)

Table 5 $P\{\tau_{D_{PL}} \leq b\}$ for regions with piecewise linear boundaries(standard errors are in parentheses)

Regions	Line segment	Quadrilateral region	Hexagon region	Region with piecewise linear boundaries	
$(t, l_1(t))$	(1.5,-0.5)	(2.5,-2)	(3,0)	(3.5,-3)	(5,0.7)
$(t, l_2(t))$	(1.5,0.5)	(2.5,1)	(3,0.8)		(5,2)
$P\{\tau_{D_{PL}} \leq b\}$	0.316909	0.808768 (0.001147)	0.828986 (0.001108)	-	0.920376 (0.002454)
$p_1^{PL}(t)$	0.316909	0.316909	0.316909	-	0.316909
$p_2^{PL}(t)$	0	0.282481 (0.000471)	0.283099 (0.000471)	-	0.316352 (0.001014)
$p_3^{PL}(t)$	0	0.209378 (0.000676)	0.228978 (0.000637)	-	0.287116 (0.001439)

and the probability that the sample path of a Brownian motion hits the region from the left boundary tends to a constant. Furthermore, from Table 1, we can obtain the probability that the sample path of a Brownian motion cannot hit a region forever, for example, for region $D_R := \{(t, X)|2 \leq t \leq 3, 0.2 \leq X \leq 1\}$, $P\{\tau_{D_R} = \infty\} \approx 0.472331$.

The numerical results of the probability $P\{\tau_{D_R} \leq b\}$ for rectangle regions with fixed $a = 2, b = 3, d = 2$ and different c are given in Table 2, which shows that the probability becomes more and more stable with the decrease of c, and the probability that the sample path of a Brownian motion hits the region from the lower boundary tends to 0.

For the case of different rectangle regions with fixed $a = 1, c = 1, d = 2$ and different b, the numerical results are given in Table 3. From Table 3, we can find that when $a = b = 1$, $P\{\tau_{D_R} \leq b\}$ is the boundary crossing probability of a standard Brownian motion and line segment $\{(t, X)|t = 1, 1 \leq X \leq 2\}$, which is in line with $p_1^R(t) = \Phi(2) - \Phi(1)$. Moreover, the probability $P\{\tau_{D_R} \leq b\}$ is increasing with the increase of b, and if $b = 10^{12}$, it can be guaranteed that the probability of a standard Brownian motion hitting the rectangle region achieves 0.999999.

From Tables 1, 2 and 3, we can get a conclusion that the size of the region has an effect on the probability, i.e., the area has a direct influence on the probability.

In order to explore the influence of position of regions on the first hitting time distribution, we calculate the probability $P\{\tau_{D_R} \leq b\}$ for rectangle regions with fixed area and different positions, without loss of generality, we let the area be 1, and the numerical results

Table 6 $P\{\tau_{D_{GN}} \leq b\}$ for regions with general nonlinear continuous boundaries(standard errors are in parentheses)

$l_1(t)/l_2(t)$	UB_1/UB_2	LB_1/LB_2	UB_1/LB_2	LB_1/UB_2	*max-min*
$P\{\tau_{D_{GN}} \leq b\}$	0.578027	0.568490	0.577764	0.569612	0.009537
	(0.001092)	(0.001132)	(0.001133)	(0.001082)	
$p_1^{GN}(t)$	0.327630	0.327630	0.327630	0.327630	0
$p_2^{GN}(t)$	0.233449	0.224445	0.233838	0.225034	0.009393
	(0.001079)	(0.001082)	(0.001078)	(0.001082)	
$p_3^{GN}(t)$	0.016948	0.016415	0.016295	0.016948	0.000653
	(0.000013)	(0.000053)	(0.000053)	(0.000003)	

are given in Table 4. From Table 4, we can find that the closer the rectangle is from the origin, the greater the probability $P\{\tau_{D_R} \leq b\}$ is; thus, the position has a significant impact on the probability.

Secondly, we give the numerical computations of the first hitting time distributions of a Brownian motion and regions of piecewise linear boundaries. We put different results involving different regions in the same table. As shown in Table 5, the double-headed arrows denote that there is an edge joining two points, for example, "$(1.5, -0.5) \leftrightarrow (2.5, -2) \leftrightarrow (3, 0)$" denotes a polygonal boundary which consists of two edges which join $(1.5, -0.5)$ and $(2.5, -2)$, $(2.5, -2)$ and $(3, 0)$, respectively; therefore, from the second row of Table 5, we can get four different forms of polygonal boundaries. And from the third row of Table 5, we can get three different forms of polygonal boundaries. The second column is the boundary crossing probability of a standard Brownian motion and line segment $\{(t, X)|t = 1.5, -0.5 \leq X \leq 0.5\}$. The third column is the probability of a standard Brownian motion hitting a quadrilateral region. The fourth column is the probability of a standard Brownian motion hitting a hexagon region. And the last column is the probability of a standard Brownian motion hitting a region with piecewise linear boundaries, where the number of the vertices of lower boundary $l_1(t)$ is more than that of upper boundary $l_2(t)$.

Finally, we give the numerical computations of the first hitting time distributions of a Brownian motion and the regions with general nonlinear continuous boundaries. The region with nonlinear continuous boundaries is given by $D_{GN} := \{(t, X)|a \leq t \leq b, l_1(t) \leq X \leq l_2(t)\}$, where $a = 1$, $b = 4$, $l_1(t) = 0.2(t^2 + 1)$ and $l_2(t) = \sqrt{0.5 + 4t}$. To obtain the estimates, 64 partition points are used. Because there are upper and lower bounds (UP and LP) for $l_1(t)$ and $l_2(t)$, we present four forms of numerical results using the computation methods of the upper and lower bounds, which is given by Wang and Pötzelberger (1997), as shown in Table 6. Obviously, the difference among the four forms of numerical results is small (*max-min*).

5 Conclusion

The calculation of the first hitting time distribution is important and attracts a great deal of interests of scientists. Explicit formulas of the first hitting time distribution of a standard Brownian motion and regions which include rectangular, triangle, quadrilateral, rhombus and a region with piecewise linear boundaries are obtained, and using these formulas, we can calculate the probability that the sample path of a Brownian motion hit a region and the probability that the sample path of a Brownian motion cannot hit a region forever. Moreover, approximations to the first hitting time distribution of a standard Brownian motion with respect to regions with general nonlinear continuous boundaries are also obtained. By combing the relationship between formulas, the relationships among the first hitting time distributions are obtained. Some existing results can be viewed as special cases of our formulas, such as the cases of one-sided piecewise linear boundaries (Wang and Pötzelberger 1997), one-sided linear boundaries (Doob (1949)) and one-sided constant boundaries (Cox and Miller 1977). Also, some numerical examples are given to illustrate the results by use of Monte Carlo simulations, and the calculation of the first hitting time distributions is simple and easy to implement. The simulation results show that both area and position have impacts on the probability that the sample path of a Brownian motion hit a region. Moreover, these formulas can be extended to compute the first hitting time distributions of a Brownian motion with linear drift with respect to regions.

Acknowledgments The research was supported by the National Natural Science Foundation of China under Grant 71631001.

References

Abundo M (2002) Some conditional crossing results of Brownian motion over a piecewise-linear boundary. Stat Prob Lett 58(2):131–145

Che X, Dassios A (2013) Stochastic boundary crossing probabilities for the Brownian motion. J Appl Probab 50(2):419–429

Cox DR, Miller HD (1977) The theory of stochastic processes. CRC Press, Boca Raton

Cui LR, Huang JB, Li Y (2016) Degradation models with wiener diffusion processes under calibrations. IEEE Trans Reliab 65(2):613–623

Daniels HE (1969) The minimum of a stationary Markov process superimposed on a U-Shaped trend. J Appl Probab 6(2):399–408

Daniels HE (1996) Approximating the first crossing-time density for a curved boundary. Bernoulli 2(2):133–143

Donchev DS (2010) Brownian motion hitting probabilities for general two-sided square-root boundaries. Methodol Comput Appl Probab 12(2):237–245

Dong QL, Cui LR (2017) A study on stochastic degradation process models under different types of failure thresholds. (Submitted)

Doob JL (1949) Heuristic approach to the Kolmogorov-Smirnov theorems. Ann Math Stat 20(3):393–403

Durbin J (1971) Boundary-crossing probabilities for the Brownian motion and Poisson processes and techniques for computing the power of the Kolmogorov-Smirnov test. J Appl Probab 8(3):431–453

Durbin J, Williams D (1992) The first-passage density of the Brownian motion process to a curved boundary. J Appl Probab 29(2):291–304

Ferebee B (1983) An asymptotic expansion for one-sided Brownian exit densities. Zeitschrift Für Wahrscheinlichkeitstheorie Und Verwandte Gebiete 63(1):1–15

Fu JC, Wu T (2010) Linear and nonlinear boundary crossing probabilities for Brownian motion and related processes. J Appl Probab 47(4):1058–1071

Gao HD, Cui LR, Kong DJ (2017) Reliability analysis for a Wiener degradation process model under changing failure thresholds. Submitted

Giraudo MT, Sacerdote L (1999) An improved technique for the simulation of first passage times for diffusion processes. Commun Stat Simul Comput 28(4):1135–1163

Giraudo MT, Sacerdote L, Zucca C (2001) A Monte Carlo method for the simulation of first passage times of diffusion processes. Methodol Comput Appl Probab 3(2):215–231

Herrmann S, Tanré E. (2016) The first-passage time of the Brownian motion to a curved boundary: an algorithmic approach. SIAM J Sci Comput 38(1):A196–A215

Jin Z, Wang L (2017) First passage time for Brownian motion and piecewise linear boundaries. Methodol Comput Appl Probab 19:237–253

Karatzas I, Shreve SE (1991) Brownian motion and stochastic calculus. Springer, New York

Kong DJ, Balakrishnan N, Cui LR (2017) Two-phase degradation process model with abrupt jump at change point governed by wiener process. IEEE Trans Reliab 66(4):1345–1360

Molini A, Talkner P, Katul GG et al (2011) First passage time statistics of Brownian motion with purely time dependent drift and diffusion. Physica A: Stat Mech Appl 390:1841–1852

Niederreiter H (1992) Random number generation and quasi-Monte Carlo methods. Society for Industrial and Applied Mathematics, Philadelphia

Novikov A, Frishling V, Kordzakhia N (1999) Approximations of boundary crossing probabilities for a Brownian motion. J Appl Probab 36(4):1019–1030

Peškir G, Shiryaev AN (1998) On the Brownian first-passage time over a one-sided stochastic boundary. Theory Prob Appl 42(3):444–453

Pötzelberger K, Wang L (2001) Boundary crossing probability for Brownian motion. J Appl Probab 38(01):152–164

Ripley BD (1987) Stochastic simulation. Wiley, New York

Siegmund D (1986) Boundary crossing probabilities and statistical applications. Ann Stat 14(2):361–404

Strassen V (1967) Almost-sure behavior of sums of independent random variables and martingales. Berkeley symposium on mathematical statistics & probability. The Regents of the University of California

Vondraček Z (2000) Asymptotics of first-passage time over a one-sided stochastic boundary. J sTheor Probab 13(1):279–309

Wang L, Pötzelberger K (1997) Boundary crossing probability for Brownian motion and general boundaries. J Appl Probab 34(1):54–65

Wang L, Pötzelberger K. (2007) Crossing probabilities for diffusion processes with piecewise continuous boundaries. Methodol Comput Appl Probab 9(1):21–40

Wang J, Zhao X, Guo X et al (2018) Analyzing the research subjects and hot topics of power system reliability through the Web of Science from 1991 to 2015. Renew Sust Energ Rev 82:700–713

Zhao X, Guo X, Wang X (2018) Reliability and maintenance policies for a two-stage shock model with self-healing mechanism. Reliability Engineering & System Safety, 172